

Krzysztof LIGIER*, Jerzy NAPIÓRKOWSKI**, Magdalena LEMECHA***

ANALYSIS OF THE HARD-FACED MULTI-PHASE MATERIAL WEAR PROCESS BY THE BALL-CRATERING METHOD

ANALIZA PROCESU ZUŻYWANIA NAPAWANYCH MATERIAŁÓW WIELOFAZOWYCH METODĄ BALL-CRATERING

Key words: abrasive wear, hard-faced multi-phase layers, ball-cratering method.

Abstract: This paper presents the results of tribological testing performed on multi-phase layers produced by the hard-facing method. Three materials based on Fe-C-Cr alloys and containing carbide-forming elements B, V, Nb, Mn, Mo and W, used to hard-face abrasion-resistant layers, were selected for the study. The ball-cratering method performed the tests in two variants: with or without an abrasive slurry. The obtained results demonstrated that all test materials showed similar wear intensity in the presence of abrasive slurry, while the wear intensity varied for the test with no abrasive slurry.

Słowa kluczowe: zużycie ściernie, wielofazowe warstwy napawane, metoda ball-cratering.

Streszczenie: W pracy przedstawiono wyniki badań tribologicznych warstw wielofazowych wykonanych metodą napawania. Do badań wybrano trzy materiały na bazie stopów Fe-C-Cr zawierających pierwiastki węglotwórcze B, V, Nb, Mn, Mo i W, stosowane do napawania warstw odpornych na ścieranie. Badania przeprowadzono metodą ball-cratering w dwóch wariantach: z obecnością zawiesiny ścierniej i bez zawiesiny ścierniej. Uzyskane wyniki wykazały, że w obecności zawiesiny ścierniej wszystkie badane materiały charakteryzowały się podobną intensywnością zużycia, natomiast w badaniu bez zawiesiny ścierniej intensywność zużycia była zróżnicowana.

INTRODUCTION

The currently applied laboratory wear testing methods offer a wide range of possibilities for selecting an appropriate tribological combination and tribological test conditions, depending on the wear process. This particularly applies to tests performed on various material and lubricant combinations. However, for abrasive wear testing in the presence of loose abrasive grains and abrasive

mass, dry abrasive-rubber wheel-type methods are commonly used (ASTM G-65 and GOST 23.208-79). Moreover, test stands are constructed to demonstrate the operating conditions, e.g., the “rotating bowl” [L. 1, 2] and “ground tunnelling” [L. 3]. In addition to laboratory methods, in-service tests [L. 4] are also used; however, they are time-consuming and make it difficult to maintain fixed testing conditions, which in particular applies to maintaining fixed properties of the abrasive mass.

* ORCID: 0000-0003-1348-7068. University of Warmia and Mazury in Olsztyn, Faculty of Technical Sciences, Oczapowskiego 11 Street, 10-719 Olsztyn, Poland. Correspondence address: e-mail: krzysztof.ligier@uwm.edu.pl.

** ORCID: 0000-0003-2953-7402. University of Warmia and Mazury in Olsztyn, Faculty of Technical Sciences, Oczapowskiego 11 Street, 10-719 Olsztyn, Poland.

*** ORCID: 0000-0003-3414-4099. University of Warmia and Mazury in Olsztyn, Faculty of Technical Sciences, Oczapowskiego 11 Street, 10-719 Olsztyn, Poland.

For this reason, test methods that enable a quick assessment of the intensity of abrasive wear of the material-material combination in the presence of abrasive are constantly being sought. One such method is the ball-cratering method, which is widely used to assess the abrasive wear intensity and abrasive wear resistance of a wide range of construction materials, i.e. metals [L. 5, 6, 7], ceramics [L. 8, 9, 10, 11], polymers [L. 12, 13, 14] as well as thin coatings [L. 15, 16, 17], including paint coatings [L. 18]. The advantage of this method is the formation of small marks of wear, which are used to determine the abrasive wear intensity. Building on the accuracy and effectiveness of this test, researchers [L. 19, 20, 21, 22, 23] modify the tester and the test procedure by introducing additional equipment for friction measurements and wear process analysis as a supplement to the ongoing research.

The materials of the hard-faced layers usually have a heterogeneous microstructure, and the resistance of these layers to abrasive wear is the sum of the resistance of the individual components. The implication is that wear resistance is determined by the number of phases and their individual characteristics. As regards iron alloys, it is mainly

the carbide phases that are involved. In addition to the carbides, the functional properties of the padding welds are also determined by the form of the matrix in which they are distributed. Due to the heterogeneous microstructure of hard-faced layers, assessing their wear resistance can be problematic, particularly when the applied test method does not allow a representative area of the padding weld to be covered by tests.

The study aimed to determine the suitability of the ball-cratering method for assessing the intensity of abrasive wear of materials with the multi-phase microstructural structure.

TEST MATERIALS

Three materials for the testing were selected for producing hard-faced layers resistant to wear in the presence of abrasive mass (El Hard 67, XHD 6715, and 6070N). The materials were deposited by the arc hard-facing method using a covered electrode onto a washer made from Hardox 500 steel. The hard-facing parameters were applied as recommended by manufacturers of the individual electrodes. The chemical composition of the selected materials is provided in **Table 1**.

Table 1. The chemical composition of the test materials

Tabela 1. Skład chemiczny badanych materiałów

Material	C	Mn	Si	Cr	Mo	W	V	Nb
El-Hard 67	5.00		1.00	23.00			10.00	
XHD 6715	5.20	0.30	1.20	17.30	5.20	3.30	0.80	5.10
6070 N	6.00	2.50	1.00	21.00	8.50	3.75	2.00	5.50

Of all the test materials, the El-Hard 67 electrode contained the least carbide-forming elements, i.e., Cr (23%) and V (10%). The other two materials contained more elements of that type. In its composition, highly carbide-forming and high-melting additives of Mn, Mo, W and Nb were found in addition to Cr and V. The contents of these elements in these padding welds differed slightly.

Specimens were taken from hard-faced metal sheets by the high-energy waterjet-cutting method and then subjected to finishing using a surface grinder and grinding-in, which gave them a cuboid shape with dimensions of 25x30x10 mm.

The assessment of the microstructure of the produced hard-faced layers was conducted by the SEM microscopy method using a Phenom XL microscope. Before the microstructure assessment, the specimen surfaces were etched with C_2H_5OH solution prepared using 3g $FeCl_3$ and 10 mL HCl.

The microstructures of the hard-faced surface layers are shown in **Figs. 1–3**.

Due to the similar chemical composition of the materials 6715 XHD and 6070N, the microstructures of these materials are also very similar and contain large precipitates of primary chromium carbides and finer niobium carbides. On the other hand, in the microstructure of the El-Hard 67 padding weld,

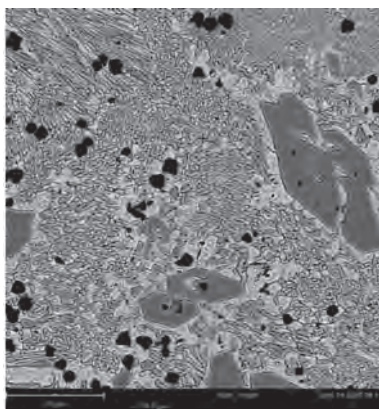


Fig. 1. Microstructure of El-Hard 67 padding weld: alloy ferrite with primary precipitates of chromium carbides and fine vanadium carbides

Rys. 1. Mikrostruktura napoiny El-Hard 67: ferryt stopowy z pierwotnymi wydzieleniami węglików chromu i drobnymi węglnikami wanadu

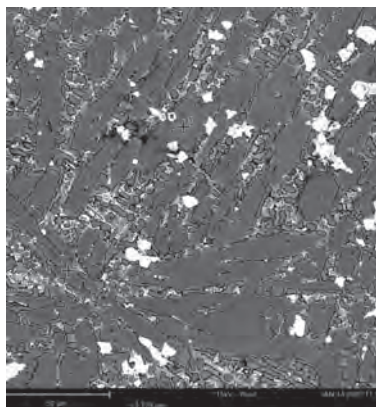


Fig. 2. Microstructure of the padding weld 6715XHD: large precipitation of primary chromium carbides and niobium carbides in the alloy ferrite matrix

Rys. 2. Mikrostruktura napoiny 6715XHD: duże wydzielenia pierwotnych węglików chromu oraz węglnikami niobu w osnowie ferrytu stopowego

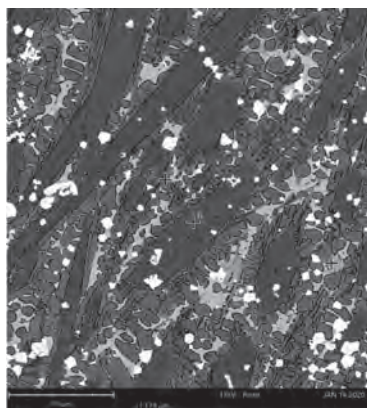


Fig. 3. Microstructure of the padding weld 6070 N: a mixture of alloy ferrite, chromium carbides and niobium carbides

Rys. 3. Mikrostruktura napoiny 6070 N: mieszanina ferrytu stopowego, węglików chromu i węglików niobu

in addition to the primary chromium carbides, fine vanadium carbides can be seen. The measurement of microhardness of the phases identified in the microstructures was performed by the Vickers method in accordance with standard PN EN ISO 6507-1, using an INNOVATEST 400-DAT-type hardness tester.

TESTING METHODOLOGY

The study employed the ball-cratering method. The tests were performed using a T-20-type tribometer (Fig. 4). A 25.4 mm (1") ball made of 100Cr6 steel was used as the counter specimen.

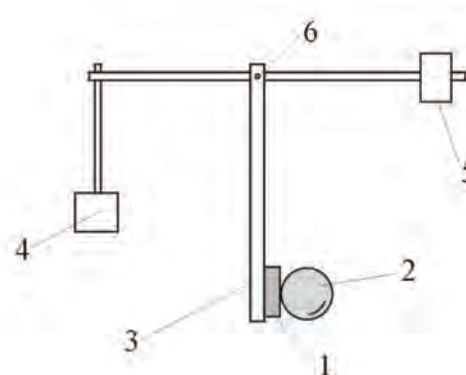


Fig. 4. Scheme and general view of the T-20 stand for testing the abrasive wear using the ball-cratering method: 1 – sample, 2 – ball (counter-sample), 3 – sample holder arm, 4 – load, 5 – counterweight, 6 – pivot

Rys. 4. Schemat i widok ogólny stanowiska T-20 do badania szybkości zużycia ściernego metodą ball-cratering: 1 – próbka, 2 – kulka (przeciwpróbka), 3 – ramię uchwytu próbki, 4 – obciążenie, 5 – przeciwważ, 6 – sworzeń.

The tests were carried out based on the standard EN-1071-6:2007. The following testing parameters were applied:

- friction assembly load: 0.4 N;

- counter specimen rotational speed: 180 rpm;
- number of revolutions: 21600;
- friction distance: 1722.73 m;
- single test duration: 2 hours.

The study was carried out in two variants:

- under technically dry friction conditions; and
- in the presence of abrasive slurry.

The abrasive slurry was alundum (Al_2O_3) with a density of 3.95 g/cm^3 and grain size of $3 \mu\text{m}$ ($\pm 1\%$) (F1200 according to FEPA – Federation of European Producers of Abrasives). A slurry volume concentration of approx. 10%, obtained by mixing 40 g Al_2O_3 in 100 cm^3 of distilled water, was used. The slurry was fed onto the friction assembly at $2 \text{ cm}^3/\text{min}$. The tests were conducted in six replications for each material, with identical test parameters. Before and after each test run, the specimen and the ball were thoroughly cleaned and degreased using ethanol.

The wear assessment was carried out based on the size of the formed craters, measured using a Keyence VHX 7000 digital optical microscope. The crater diameter was measured in the directions parallel and perpendicular to the direction of ball rotation.

The tests were conducted in the variant with no coating perforation. The wear volume was determined using the formula:

$$V = \frac{\pi b^4}{64 \cdot R}$$

where:

R – ball radius,

b – mean crater diameter.

Based on the calculated volume, the intensity of material wear was determined using the Archard equation, which relates the wear volume V to the normal load N and the sliding distance S, from the formula:

$$K_c = \frac{\pi b^4}{64 R S N}$$

where:

K_c – coating abrasive wear intensity,

R – ball radius,

b – mean crater diameter,

S – friction distance,

N – normal load.

TEST RESULTS

The results of testing for microhardness of the hard-faced layers are shown in **Table 2**.

As indicated by the test results, the hardness of the individual phases in the microstructure of the test layers varies. The greatest hardness of the matrix (974HV0.05) was obtained for the 6715XHD padding weld, while for the other materials, the hardness of this phase was approx. 900 HV0.05. The 6715XHD padding weld was characterised by chromium carbide hardness (1855 HV0.05) compared to the other materials (1294 – 1355 HV0.05). It should be noted that the hardness of carbide precipitates showed high variability, as evidenced by the range values.

An example of the crater obtained during the testing is presented in **Fig. 5**.

Table 2. Microhardness of the tested hard-faced layers

Tabela 2. Mikrotwardość badanych warstw napawanych

Material	Phase	Microhardness [HV 0.05] median	Range [HV 0.05]
El-Hard 67	Matrix	902	311
	Chromium carbide	1355	603
	Vanadium carbide	1017	213
6715 XHD	Matrix	974	56
	Chromium carbide	1855	687
	Niobium carbide	2273	685
6070N	Matrix	908	150
	Chromium carbide	1294	462
	Niobium carbide	1131	156

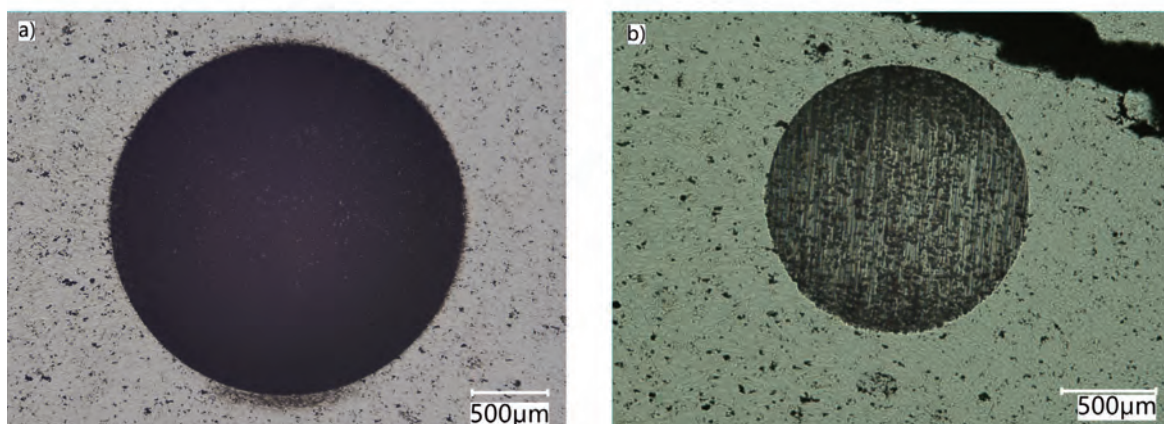


Fig. 5. Crater obtained in the 6715XHD padding weld test: a) in the presence of abrasive slurry, b) under dry friction conditions

Rys. 5. Krater uzyskany w badaniu napoiny 6715XHD: a) w obecności zawiesiny ścierniej, b) w warunkach tarcia technicznie suchego

The results of the wear intensity coefficient for the tested hard-faced layers being worn under technically dry friction conditions are shown in **Fig. 6**, while the results obtained during the tests in the presence of abrasive slurry are shown in **Fig. 7**.

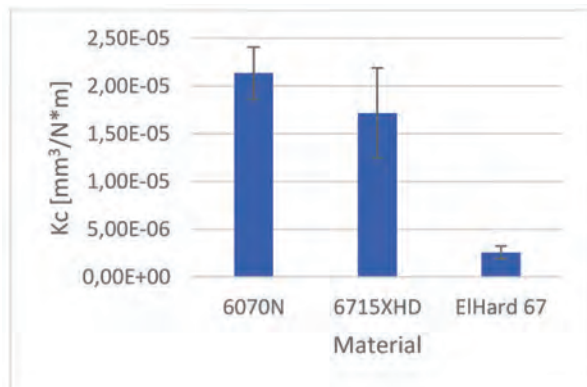


Fig. 6. Average values of the K_c index obtained in the test under the dry friction conditions. Error bars – std. dev.

Rys. 6. Wartości średnie wskaźnika K_c uzyskane w badaniu w warunkach tarcia technicznie suchego. Słupki błędów – odch. std.

As indicated by the obtained K_c coefficient values, in the testing variant under technically dry friction conditions, the 6070N and 6715XHD padding welds were characterised by a significantly higher wear rate than El-Hard 67. The K_c coefficient values for this testing variant were as follows: for the 6070N padding weld – $2.14E^{-5}$; for the 6715XHD padding weld – $1.72E^{-5}$; and for the El Hard padding weld – $2.5E^{-6}$. The value obtained for the El-Hard 67

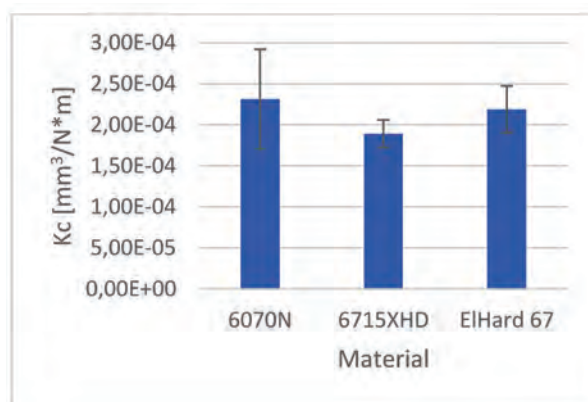


Fig. 7. Average values of the K_c index obtained in the test in the presence of abrasive slurry. Error bars – std. dev.

Rys. 7. Wartości średnie wskaźnika K_c uzyskane w badaniu w obecności zawiesiny ścierniej. Słupki błędów – odch. std.

padding weld is approx. ten times lower than that for the 6070N padding weld. The K_c coefficient values for the tested padding welds were similar in the testing variant, including abrasive slurry. Notably, there is a significant scattering of the K_c coefficient values for the individual materials, which is indicated by the error bar values. This is due to the heterogeneous microstructure of the tested materials, which resulted in craters of varying diameters being obtained in the individual test runs.

Fig. 8 shows a view of the cratered surface made in the 6070N padding weld in the non-abrasive test variant, while **Fig. 9** shows a view of the crater surface in the presence of abrasive slurry.

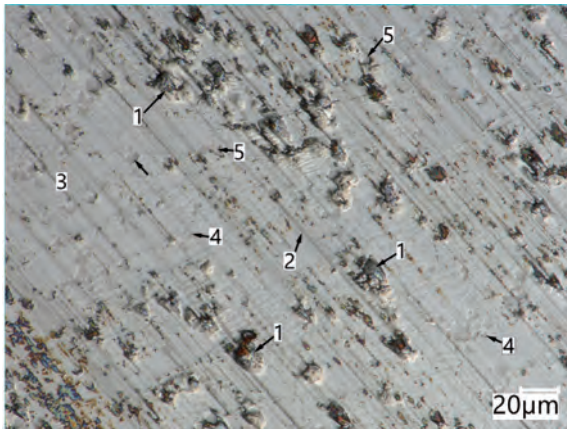


Fig. 8. The surface of the padding weld 6070N worn in dry friction conditions: 1 – point material losses, 2 – ploughing, 3 – chromium carbide, 4 – vanadium carbide

Rys. 8. Powierzchnia napoiny 6070N zużywanej w warunkach tarcia suchego: 1 – punktowe ubytki materiału, 2 – bruzdowanie, 3 – węglík chromu, 4 – węglík wanadu



Fig. 9. The surface of the padding weld 6070N worn in the presence of an abrasive slurry: 1 – ploughing, 2 – chromium carbides, 3 – vanadium carbides, 4 – niobium carbides

Rys. 9. Powierzchnia napoiny 6070N zużywanej w obecności zawiesiny ścierniej: 1 – bruzdowanie, 2 – węglíki chromu, 3 – węglíki wanadu, 4 – węglíki niobu

On the cratered surface made with no abrasive (Fig. 8), ridging marks running in the direction of relative movement and irregularly shaped spots of material losses were observed. This form of surface damage is similar to chipping. The shape of these losses indicates that they may have resulted from the shallowly embedded, fine carbide precipitates being chipped from the surface. This process was resisted, to a large extent, by fine vanadium carbide precipitates firmly embedded in the matrix and, to a lesser extent, by large chromium carbides. The cratered surface made in the presence of abrasive slurry (Fig. 9) only shows ridging marks, resulting

in the exposure of fine vanadium carbides and large chromium carbide precipitates. The grooves cut out by sharp-edged abrasive grains of Al_2O_3 have better-defined edges. No signs of chipping were identified on the surface.

The view of the cratered surface made in the 6715XHD padding weld is shown in Fig. 10 (a variant with no abrasive slurry) and Fig. 11 (a variant with an abrasive slurry).

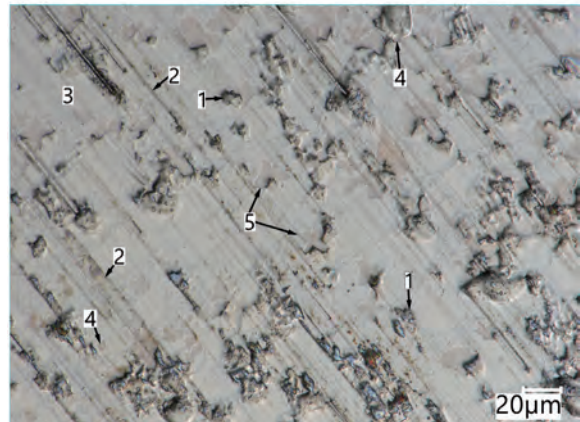


Fig. 10. The surface of the 6715XHD padding weld worn in dry friction conditions: 1 – point material losses, 2 – ploughing, 3 – chromium carbide, 4 – vanadium carbide, 5 – niobium carbide

Rys. 10. Powierzchnia napoiny 6715XHD zużywanej w warunkach tarcia suchego: 1 – punktowe ubytki materiału, 2 – bruzdowanie, 3 – węglík chromu, 4 – węglík wanadu, 5 – węglík niobu

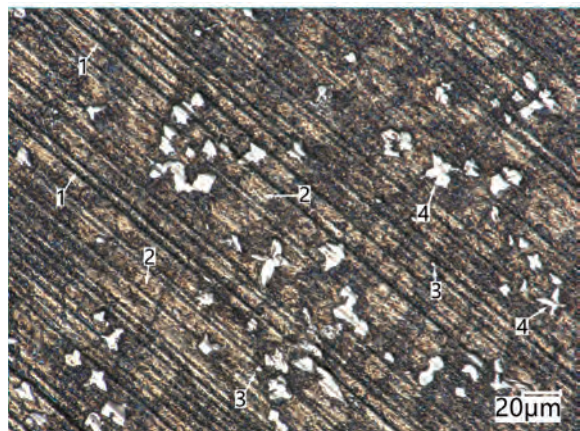


Fig. 11. The surface of the 6715XHD padding weld worn in the presence of an abrasive slurry: 1 – ploughing, 2 – chromium carbides, 3 – vanadium carbides, 4 – niobium carbides

Rys. 11. Powierzchnia napoiny 6715XHD zużywanej w obecności zawiesiny ścierniej: 1 – bruzdowanie, 2 – węglíki chromu, 3 – węglíki wanadu, 4 – węglíki niobu

As in the case of the 6070N padding weld case, the cratered surface made in the 6715XHD

weld without abrasive slurry (**Fig. 10**) exhibits ridging marks running in the relative movement direction and spots of material losses, bearing the characteristics of chipping (sharp pit edges). Fine carbide phase precipitates were chipped off. On the other hand, the cratered surface made in the presence of abrasive slurry (**Fig. 11**) bears ridging marks. The ridging mainly impacted the matrix material and, to a lesser extent, chromium carbides, while vanadium carbides and niobium carbides resisted the process. In the presence of abrasive slurry, no marks of carbides being chipped off from the padding weld surface could be observed.

Figures 12 and 13 present the view of the cratered surfaces made in the El-Hard 67 padding weld without abrasive slurry (**Fig. 12**) and in the presence of abrasive slurry (**Fig. 13**).

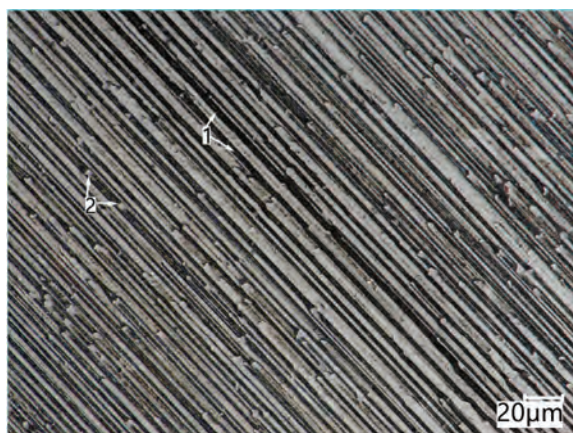


Fig. 12. The surface of the El-Hard 67 padding weld worn in dry friction conditions: 1 - ploughing, 2 - vanadium carbide

Rys. 12. Powierzchnia napoiwy El-Hard 67 zużywaney w warunkach tarcia suchego: 1 – bruzdowanie, 2 – węglik wanadu

Ridging marks can be found on the cratered surface made in the El-Hard 67 padding weld in both testing variants. On the cratered surfaces, numerous grooves can be seen, along with numerous exposed fine vanadium carbides, which are firmly embedded in the matrix. The pattern of the grooves indicates that these precipitates effectively inhibit the material removal process in the testing variant with no abrasive slurry (**Fig. 12**). In the presence of abrasive slurry, not only ridging marks but also small pits resulting from the rolling of abrasive grains along the surface of the material within the area of increased surface pressure, i.e., the so-called rolling abrasion, can be observed.

As for the testing in the presence of abrasive slurry, the ridging processes visible as grooves cut

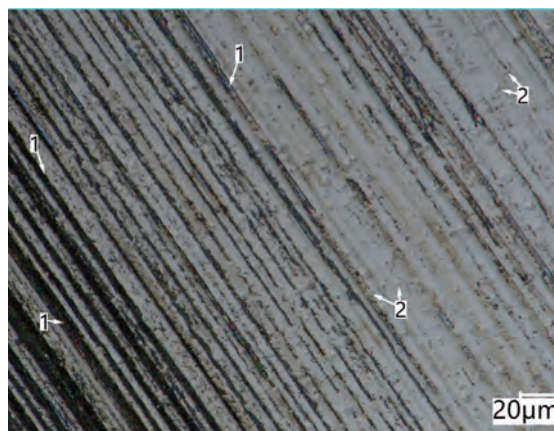


Fig. 13. The surface of the El-Hard 67 padding weld worn in the presence of abrasive slurry: 1 – ploughing, 2 – vanadium carbides

Rys. 13. Powierzchnia napoiwy El-Hard 67 zużywaney w obecności zawiesiny ścierney: 1 – bruzdowanie, 2 – węglik wanadu

out in the direction of abrasive grain movement were dominant on the surface of all materials. The ridging processes impacted the matrix and chromium carbides, while fine niobium and vanadium carbide precipitates, firmly embedded in the surface layer, resisted these processes, which resulted in their exposure. The counter specimen (ball) rested on the exposed, protruding carbides, and the abrasive grains could still penetrate between the specimen and the counter specimen and impact the other microstructure phases, resulting in their destruction. In this testing variant, the test material wear rate was similar.

CONCLUSIONS

1. The presented test results show that the hard-faced layer wear process proceeded differently depending on the testing variant. In the presence of abrasive slurry, the processes of surface ridging by abrasive grains found in the slurry were dominant. The impact of abrasive slurry resulted in material removal around fine carbides without chipping them.
2. The testing carried out under the technically dry friction conditions revealed that on the surface of materials containing less fine niobium and vanadium carbide precipitates and more large chromium carbide precipitates, not only ridging but also chipping of shallowly embedded carbides from the matrix material occurred. As for the El-Hard 67 padding weld, the presence

of a large number of fine, firmly deposited vanadium carbides in the microstructure resulted in them providing support points for the counter specimen, which reduced contact between the counter specimen and the matrix and resulted in slower wear of the material.

3. The ball-cratering method's application for assessing the abrasive wear resistance of hard-faced multi-phase layers is limited. The

limitations are due to the small area covered by the study, which, for highly heterogeneous microstructures, results in a significant scattering of results. The application of the variant, including abrasive slurry, positively contributed to the repeatability of the results, and for this reason, the methods should be employed in this variant.

REFERENCES

1. Ligier K., Napiórkowski J., Lemecha M.: The Effect Of Abrasive Mass Moisture Content On The Abrasion-Resistant Steel Wear Rate. *Quarterly Tribologia* 2019, 284 (2), pp. 75–82.
2. Napiórkowski J., Ligier K.: Tribological Properties Of Polyurethanes In Abrasive Soil Mass. *Tribologia* 276(6), pp. 65–70.
3. Alavi Gharahbagh E., Rostami J., Palomino A.M.: New Soil Abrasion Testing Method For Soft Ground Tunneling Applications. *Tunnelling and Underground Space Technology*, Vol. 26, Issue 5, pp. 604–613.
4. Napiórkowski J., Lemecha M.: An Analysis Of The Wear Of Ploughshares With Various Technological Solution. *Quarterly Tribologia* 2016, 267 (3), pp. 139–151.
5. Stachowiak G.B., Stachowiak G.W., Celliers O.: Ball-Cratering Abrasion Tests of High-Cr White Cast Irons, *Tribol. Int.*, 2005, 38, pp. 1076–1087.
6. Mathew M.T., Stack M.M., Matijevic B., Rocha L.A., Ariza E.: Micro-Abrasion Resistance of Thermochemically Treated Steels in Aqueous Solutions: Mechanisms, Maps, Materials Selection, *Tribol. Int.*, 2008, 41, pp. 141–149.
7. Marques F., da Silva W.M., Pardal J.M., Tavares S.S.M., and Scandian C., Influence of Heat Treatments on the Micro-Abrasion Wear Resistance of a Superduplex Stainless Steel, *Wear*, 2011, 271, pp. 1288–1294.
8. Vale Antunes P., Ramalho A.: Study of Abrasive Resistance of Composites for Dental Restoration by Ball-Cratering, *Wear* 2003, 255, pp. 990–998.
9. Stachowiak G.B., Stachowiak G.W.: Tribological Characteristics of WC-Based Claddings Using a Ball-Cratering Method, *Int. J. Refract. Met. H.* 2010, 28, pp. 95–105.
10. Sharifi S., Stack M.M., Stephen L., Wang-Long Li, Moo-Chin Wang: Micro-Abrasion of Y-TZP in Tea, *Wear* 2013, 297, pp. 713–721.
11. Ibañez M.J., Gilabert J., Vicent M., Go´mez P., and Muñoz D.: Determination of the Wear Resistance of Traditional Ceramic Materials by Means of Micro-Abrasion Technique, *Wear* 2009, 267, pp. 2048–2054.
12. Sampaio M., Buciumeanu M., Henriques B., Silva F. S., Souza J.C.M., Gomes J.R.: Comparison Between PEEK and Ti6Al4V Concerning Micro-Scale Abrasion Wear on Dental Applications, *J. Mech. Behav. Biomed. Mater.* 2016, 60, pp. 212–219.
13. Farfán-Cabrera L.I., Gallardo-Hernández E.A., Sedano de la Rosa C., Vite-Torres M.: Micro-Scale Abrasive Wear of Some Sealing Elastomers, *Wear* 2017, 376–377, pp. 1347–1355.
14. Ligier K., Olejniczak K., Napiórkowski J.: Wear of polyethylene and polyurethane elastomers used for components working in natural abrasive environments, *Polymer Testing*, Volume 100, 2021, 107247.
15. Batista J., Joseph M., Godoy C., Matthews A.: Micro-Abrasion Wear Testing of PVD TiN Coatings on Untreated and Plasma Nitrided AISI, H13 Steel, *Wear* 2002, 249, pp. 971–979.
16. Silva F., Martinho R., Baptista A.: Characterisation of Laboratory and Industrial CrN/CrCN/Diamond-Like Carbon Coatings, *Thin Solid Films*, 2014, 550, pp. 278–284.
17. Osuch-Słomka E., Michalczewski R., Szczerek M.: Ocena odporności na zużywanie powłok PVD/CVD metodą ball-cratering. *Tribologia* 2007, pp. 213–214 (3–4), pp. 47–58.

18. Napiórkowski J., Ligier K., Lemecha M., Fabisiak D.: Evaluation of tribological properties of powder paint coatings using the ball-cratering method. *Quarterly Tribologia* 2019, 288 (6), pp. 57–63.
19. Gee M.G. and Wicks M.J.: Ball Crater Testing for the Measurement of the Unlubricated Sliding Wear of Wear-Resistant Coatings, *Surf. Coat. Technol.* 2000, 133–134, pp. 376–382.
20. Cozza R.C.: Influence of the Normal Force, Abrasive Slurry Concentration and Abrasive Wear Modes on the Coefficient of Friction in Ball-Cratering Wear Tests, *Tribol. Int.* 2014, 70, pp. 52–62.
21. Peng Y. Ni X., Zhu Z., Yu Z., Yin Z., Li T., Liu S., Zhao L., Xu J.: Friction and Wear of Liner and Grinding Ball in Iron Ore Ball Mill, *Tribol. Int.* 2017, 115, pp. 506–517.
22. Bello J., Wood R., Wharton J.: Synergistic Effect of Micro-Abrasion-Corrosion of UNS S30403, S31603 and S32760 Stainless Steels, *Wear* 2007, 263, pp. 149–159.
23. Stack M., Rodling J., Mathew M., Jawan H., Huang W., Parck G., Hodge C.: Micro-Abrasion-Corrosion of a Co-Cr/UHMWPE Couple in Ringer's Solution: An Approach to Construction of Mechanism and Synergism Maps for Application to Bio-Implants, *Wear*, 2010, 269, pp. 376–382.